
Adapting Contrastive Language-Image Pretrained (CLIP) Models for Out-of-Distribution Detection

Nikolas Adaloglou
Heinrich Heine University, Duesseldorf

adaloglo@hhu.de

Felix Michels
Heinrich Heine University, Duesseldorf

felix.michels@hhu.de

Tim Kaiser
Heinrich Heine University, Duesseldorf

tikai103@hhu.de

Markus Kollman
Heinrich Heine University, Duesseldorf

markus.kollmann@hhu.de

Abstract

We present a comprehensive experimental study on pretrained feature extractors for visual out-of-distribution (OOD) detection, focusing on adapting contrastive language-image pretrained (CLIP) models. Without fine-tuning on the training data, we are able to establish a positive correlation ($R^2 \geq 0.92$) between in-distribution classification and unsupervised OOD detection for CLIP models in 4 benchmarks. We further propose a new simple and scalable method called *pseudo-label probing* (PLP) that adapts vision-language models for OOD detection. Given a set of label names of the training set, PLP trains a linear layer using the pseudo-labels derived from the text encoder of CLIP. To test the OOD detection robustness of pretrained models, we develop a novel feature-based adversarial OOD data manipulation approach to create adversarial samples. Intriguingly, we show that (i) PLP outperforms the previous state-of-the-art (Ming et al., 2022) on all 5 large-scale benchmarks based on ImageNet, specifically by an average AUROC gain of 3.4% using the largest CLIP model (ViT-G), (ii) we show that linear probing outperforms fine-tuning by large margins for CLIP architectures (i.e. CLIP ViT-H achieves a mean gain of 7.3% AUROC on average on all ImageNet-based benchmarks), and (iii) billion-parameter CLIP models still fail at detecting adversarially manipulated OOD images. The code and adversarially created datasets will be made publicly available.

1 Introduction

Transferring the representations of pretrained vision models has improved the performance on a plethora of image recognition tasks (Yosinski et al., 2014; Tan et al., 2018; Park et al., 2023; Adaloglou et al., 2023). To date, these models are trained with various types of supervision, which accelerates training convergence compared to random initialization (He et al., 2019). Examples include self-supervision (Chen et al., 2020b), natural language supervision (Radford et al., 2021), weakly-supervised learning (Mahajan et al., 2018), or standard supervised learning. Concurrently, Dosovitskiy et al. (2021) have established vision transformers (ViTs), along with an enormous number of variants (Liu et al., 2021; Touvron et al., 2021; Beyer et al., 2023), as a suitable architecture for training large-scale models in the visual domain (Dehghani et al., 2023).

Nevertheless, the applicability of the learned features of pretrained models is crucial and non-trivial, especially for unsupervised downstream tasks (Bommasani et al., 2021; Adaloglou et al., 2023). This work centers

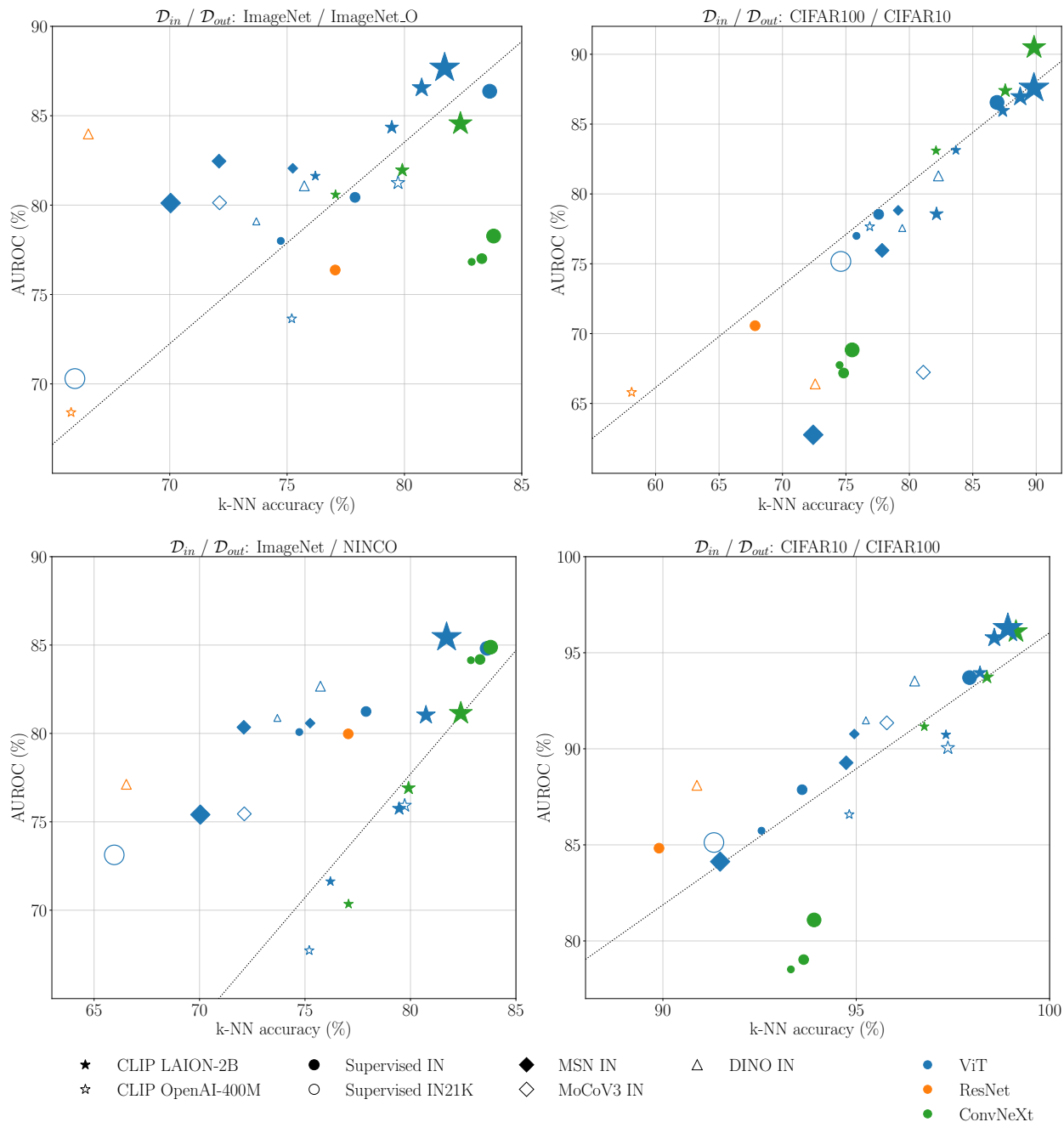


Figure 1: **In-distribution test accuracy using $k = 20$ nearest neighbours (k-NN) (x-axis) versus unsupervised out-of-distribution (OOD) detection score (AUROC %) (y-axis) for ImageNet→ImageNet-O, CIFAR100→CIFAR10, ImageNet→NINCO and CIFAR10→CIFAR100** Deng et al. (2009); Hendrycks et al. (2021b); Krizhevsky et al. (2009). CLIP models Radford et al. (2021); Cherti et al. (2022) exhibit a strong dependence between OOD performance and in-distribution test accuracy even without fine-tuning. The black dotted line is fitted using the CLIP models (starred datapoints), where a coefficient $R^2 > 0.92$ for all benchmarks was found. The OOD detection score is computed using the top-1 NN cosine similarity. Different colors are utilized for different architectures (ViT Dosovitskiy et al. (2021), ConvNeXt Liu et al. (2022), ResNet He et al. (2016)) while symbol sizes roughly indicate architecture size (i.e. Small, Base, Large, Huge, Giga). IN indicates ImageNet and IN21K indicates ImageNet-21K Russakovsky et al. (2015). Best viewed in color.

on adapting pretrained feature extractors for various visual OOD detection setups, focusing on contrastive language-image pretraining (*CLIP*) models.

The task of OOD, novelty, or anomaly detection aims at identifying whether a given test sample is drawn from the *in-distribution* (the training set) or an alternative distribution, known as the *out-distribution*. Accurate detection of anomalies is indispensable for real-world applications to ensure safety during deployment (Amodei et al., 2016; Ren et al., 2019). The detected unfamiliar samples can be processed separately, possibly with a human expert in the loop, rather than making a potentially uncalibrated prediction (Guo et al., 2017). Despite significant advances in deep learning, neural networks tend to generate systematic errors for test examples far from the training set (Nguyen et al., 2015) or assign higher likelihoods to OOD samples compared to in-distribution samples (Nalisnick et al., 2019).

Recent studies have established a firm connection between the training data distribution accuracy and OOD generalization (Hendrycks et al., 2021a; Wenzel et al., 2022; Dehghani et al., 2023). A similar connection has been identified for supervised OOD detection when in-distribution training labels are available for training or fine-tuning. Supervised training leads to intermediate representations that likely form tight label-related clusters (Fort et al., 2021). An ideal representation for OOD detection should capture semantic properties, such as the pose and shape of an object while remaining sensitive to the properties of the imaging process (e.g. lighting, resolution) (Winkens et al., 2020).

A suitable choice of visual feature representations is critical for detecting anomalies. However, learning informative representations for unsupervised OOD detection (Tack et al., 2020; Sehwan et al., 2021; Rafiee et al., 2022), where no in-distribution labels are available, is a challenging and active research area (Cohen et al., 2023). Unsupervised methods often adopt self-supervision to learn the in-distribution features by defining pretext tasks such as rotation prediction (Gidaris et al., 2018). A major milestone in visual representation learning was reached by Chen et al. (2020b) with the development of contrastive and non-contrastive visual self-supervised methods (Caron et al., 2021). Recently, CLIP has enabled learning from vast amounts of raw text (Radford et al., 2021). Vision-language models offer the unprecedented advantage of zero-shot image classification by leveraging the label names of the downstream dataset. Nonetheless, adapting CLIP models is not straightforward, even in the supervised scenario. For instance, Pham et al. (2023) showed that fine-tuning CLIP models degrades their robustness against classifying distribution-shifted samples.

Labeled OOD samples are typically unavailable in real-world applications, and the number of in-distribution samples is usually limited. Therefore, external data have been widely employed (Rafiee et al., 2022) in two ways: a) outlier exposure where the external data is treated as anomalous (Hendrycks et al., 2019a), and b) using models pretrained on auxiliary data (Sun et al., 2022). Outlier exposure leads to performance gains only if the auxiliary data are sufficiently diverse and disjoint from the in-distribution (Hendrycks et al., 2019a; Liznerski et al., 2022). On the other hand, Hendrycks et al. (2020; 2021a) showed that pretrained backbones can enhance OOD detection performance and robustness without relying on dataset-specific shortcuts (Geirhos et al., 2020). Consequently, pretrained models are suitable candidates for OOD detection, while Galil et al. (2023) has recently established CLIP models for OOD detection, especially when in-distribution label names are present (Ming et al., 2022).

In parallel, several OOD detection methods still rely on similar small-scale benchmarks based on low-resolution images (Mohseni et al., 2021; Rafiee et al., 2022; Esmailpour et al., 2022), such as CIFAR (Krizhevsky et al., 2009). Huang & Li (2021) argued that methods explicitly tuned for these benchmarks may not always translate effectively into larger-scale and real-life applications. Towards this direction, new large-scale and more challenging benchmarks have been introduced (Hendrycks et al., 2021b; Yang et al., 2022; Bitterwolf et al., 2023), which consider ImageNet (Deng et al., 2009) as in-distribution. Finally, even though the robustness against adversarial attacks has been sufficiently explored in image classification (Szegedy et al., 2014; Goodfellow et al., 2015; Mao et al., 2023), less attention has been given to studying the construction of robust visual OOD detectors (Azizmalayeri et al., 2022; Yin et al., 2021). Even though several advancements in visual feature extractors have been made and new large-scale OOD detection benchmarks (Bitterwolf et al., 2023) have been proposed, limited research has been conducted in OOD detection regarding the choice of pretrained model and evaluation scheme, especially regarding CLIP models (Ming et al., 2022; Galil et al., 2023; Esmailpour et al., 2022).

In this paper, we present an experimental study across 25 feature extractors and several visual OOD detection benchmarks. Using the existing publicly available models, we demonstrate that large-scale CLIP models are robust unsupervised OOD detectors and focus on adapting the representations of CLIP under different OOD detection settings. Under this scope, we examine several OOD detection setups based on the availability of labels or image captions (i.e. in-distribution class names). The core contributions of this work are summarized as follows:

- To investigate whether the dependence between in-distribution accuracy and unsupervised OOD detection performance can be confirmed without in-distribution fine-tuning, we quantify the performance of 25 pretrained models across 4 benchmarks (Fig. 1). CLIP models exhibit the strongest positive correlation without fine-tuning across all benchmarks (R^2 coefficient ≥ 0.92). Interestingly, the features of CLIP ViT-G outperform the ones from supervised ImageNet pretraining on ImageNet-based OOD detection.
- To adapt the representations of CLIP for OOD detection, we propose a simple and scalable method called pseudo-label probing (PLP). Here, text-based pseudo-labels are computed using its text encoder based on the maximum image-text feature similarity. We leverage the obtained text-based pseudo-labels to train a linear layer on top of CLIP. PLP surpasses the previous state-of-the-art (Ming et al., 2022) on 5 ImageNet benchmarks by an average AUROC gain of 1.8% and 3.4% for CLIP ViT-H and CLIP ViT-G, respectively. Moreover, linear probing achieves superior performance on ImageNet-based OOD benchmarks compared to fine-tuning, notably by a mean AUROC gain of 7.3% using CLIP ViT-H.
- Finally, we introduce a novel method that adversarially manipulates OOD images by matching their representations to in-distribution samples and confirm that CLIP ViT-G trained on billions of samples can be easily fooled (86.2% \rightarrow 50.3% AUROC deterioration), by changes that are invisible to humans.

2 Related work

2.1 Supervised OOD detection methods

Supervised OOD detection methods rely on the fact that in-distribution classification accuracy is positively correlated with OOD detection performance (Fort et al., 2021; Galil et al., 2023). For that reason, many OOD detection methods derive anomaly scores from supervised in-distribution classifiers. Hendrycks & Gimpel (2017) developed the maximum softmax probability (MSP) as OOD detection score, which is frequently used, or its temperature scaled version (Liang et al., 2018). More recently developed scores based on the logits of the in-distribution classifier are the maximum logit (Hendrycks et al., 2022) or the negative energy scores by Liu et al. (2020). An alternative OOD detection score, which requires the in-distribution labels, is the parametric Mahalanobis-based score (Lee et al., 2018). The Mahalanobis score assumes that the representations from each class are normally distributed around the per-class mean and conform to a mixture of Gaussians (Ren et al., 2021; Fort et al., 2021). Later on, Sun et al. (2022) established an important yet simple OOD detection score, namely the k -nearest neighbors (NN) distance, without requiring the feature norms (Tack et al., 2020) or temperature tuning (Rafiee et al., 2022). The k -NN distance has the advantage of being non-parametric and model- and distribution-agnostic.

Supervised learning may not always produce sufficiently informative features for identifying OOD samples (Winkens et al., 2020). To this end, additional tasks have been proposed to enrich the supervised-learned features. Examples include determining the key in-distribution transformations and predicting them (Hendrycks et al., 2019b) or contrastive learning. Mohseni et al. (2021) attempt to first learn the domain-specific transformations for each in-distribution using Bayesian optimization. Zhang et al. (2020) present a two-branch framework, where a generative flow-based model and a supervised classifier are jointly trained.

2.2 Unsupervised OOD detection methods

Unsupervised OOD detection methods rely on learning in-distribution features, typically accomplished with contrastive or supervised contrastive learning (Sehwag et al., 2021; Khosla et al., 2020). Contrastive-based methods can be further enhanced by designing hand-crafted transformations that provide an estimate of near OOD data (Rafiee et al., 2022) or by developing better OOD detection scores Tack et al. (2020). For example, Tack et al. (2020) add a transformation prediction objective (i.e. rotation prediction such as $[0^\circ, 90^\circ, 180^\circ, 270^\circ]$). Sehwag et al. (2021) define a simpler contrastive-based OOD detection method, where the Mahalanobis distance is computed in the feature space using the cluster centers of k -means (Lloyd, 1982).

2.3 OOD detection methods using external data or pretrained models

Early works attempted to use external data to generate examples near the OOD decision boundary or incorporate them for outlier exposure and negative sampling (Hendrycks et al., 2019a; Rafiee et al., 2022). Nonetheless, disjointness between the in and out-distribution cannot be guaranteed, and applying shifting transformations depends on the in-distribution (Mohseni et al., 2021), which limits the applicability of such approaches.

Hendrycks et al. (2020) show that large-scale models pretrained on diverse external datasets can boost OOD detection performance. Recent OOD detection scores, which leverage pretrained models, deal with the large semantic space by, for instance, grouping images with similar concepts into small groups as in Huang & Li (2021). The majority of existing methods focus on supervised OOD detection (Sun et al., 2022; Galil et al., 2023). Such approaches include fine-tuning the whole network or parts of it (Reiss et al., 2021). Contrarily, Ren et al. (2021) showed that a Mahalanobis-based score could achieve comparable OOD detection performance on small-scale benchmarks without fine-tuning.

Out of the limited label-free methods based on pretrained models, a simple approach is the k -NN feature similarity, which has not been studied systematically across pretrained models (Sun et al., 2022). Another unsupervised approach aims at initially detecting an *a priori* set of visual clusters. The obtained clusters are subsequently used as pseudo-labels for fine-tuning (Cohen et al., 2023). Apart from unsupervised OOD detection, CLIP models can additionally leverage in-distribution class names (Esmailpour et al., 2022), and in-distribution prototypes can be obtained using the textual encoder, which has not been thoroughly investigated. Esmailpour et al. (2022) extend the CLIP framework by training a text-based generator on top, while Ming et al. (2022) compute the maximum softmax probability of image-text feature similarities. Approaches that would alleviate the need to fine-tune billion-scale models remain relatively unexplored, especially in conjunction with CLIP models Wortsman et al. (2022).

2.4 OOD detection robustness

Hendrycks & Dietterich (2019) analyzed the robustness under corruptions and geometric perturbations, such as Gaussian noise and brightness shift. Since it is not always clear which manually perturbed images are present in the in-distribution and which are not, attention has been given to adversarial robustness (Chen et al., 2020a). Existing works have primarily focused on fooling supervised OOD detection methods on small-scale benchmarks (Yin et al., 2021). Despite the fact that CLIP models’ zero-shot classification performance deteriorates significantly when the input images are constructed adversarially (Mao et al., 2023), their adversarial OOD detection robustness has not been thoroughly investigated.

3 The proposed OOD detection setup

3.1 Considered pretrained models

Several supervised CNNs, such as ResNet50 (He et al., 2016), ConvNext (Liu et al., 2022) and ViT (Dosovitskiy et al., 2021) models trained on ImageNet and ImageNet-21K (Deng et al., 2009; Russakovsky et al., 2015) were utilized. Regarding Imagenet-pretrained self-supervised models, the DINO (Caron et al., 2021), MoCov3 (Chen et al., 2021), and MSN (Assran et al., 2022) were selected. Finally, CLIP-based models were either

Architecture	Images/ second	Number of Params (M)
ResNet50	2719	24
ConvNext-S	1576	49
ConvNext-B	1157	88
ConvNext-L	695	196
ConvNext-B wide	888	88
ConvNext-L deep	531	200
ConvNext-XXL	180	847
ViT-S/16	3210	22
ViT-B/16	1382	86
ViT-L/16	475	303
ViT-H/14	183	631
ViT-G/14	78	1843

Table 1: **Number of parameters (in millions) and inference time (images per second on a single GPU) for the utilized network architectures.**

Dataset	Classes	Train images	Validation images
<i>Pretraining datasets</i>			
ImageNet	1K	1.28M	-
ImageNet-21K	21K	14M	-
OpenAI-400M	-	400M	-
LAION-2B	-	2B	-
<i>In-distribution datasets</i>			
CIFAR10	10	50K	10K
CIFAR100	100	50K	10K
ImageNet	1K	1.28M	50K
<i>Out-distribution datasets</i>			
iNaturalist	110	-	10K
SUN	50	-	10K
Places	50	-	10K
IN-O	200	-	2K
NINCO	64	-	5.88K
Texture	47	-	5.54K
CIFAR10-A	10	-	1000
CIFAR10-AS	10	-	1000

Table 2: **An overview of the number of classes and the number of samples on the considered datasets.**

trained on OpenAI-400M (Radford et al., 2021) or LAION-2B (Schuhmann et al., 2022), which consists of 400M and 2 billion image-text description pairs, respectively. Further information regarding the network complexities is reported in Tab. 1. To quantify the complexity, we performed inference on a single GPU with a batch size of 256 to compute the images per second that were processed at 224×224 resolution.

3.2 Datasets and metrics

We denote the in-distribution as \mathcal{D}_{in} , and the out-distribution as \mathcal{D}_{out} . The corresponding train and test splits are indicated with a superscript. To design a fair comparison between vision and vision-language models, we define *unsupervised OOD detection* without having access to the set of \mathcal{D}_{in} label names. Following Huang & Li (2021), we use ImageNet as \mathcal{D}_{in} for large-scale OOD detection benchmarks and CIFAR for small-scale benchmarks.

For the large-scale benchmarks, we use the following 5 OOD datasets: Imagenet-O (IN-O) (Hendrycks et al., 2021b), a flower-based subset of iNaturalist (Van Horn et al., 2018), Texture (Cimpoi et al., 2014), a subset of the SUN scene database (Xiao et al., 2010), a subset of Places (Zhou et al., 2017). IN-O contains 2K samples from ImageNet-21K, excluding ImageNet. It is worth noting that Places, Textures, and IN-O have a class overlap of 59.5%, 25.6%, and 20.5% with ImageNet, according to Bitterwolf et al. (2023). Therefore, we additionally use the newly proposed NINCO Bitterwolf et al. (2023), which contains 5879 samples belonging to 64 classes with zero class overlap with ImageNet’s classes. Dataset information is summarized in Tab. 2.

To quantify the OOD detection performance, the area under the receiver operating characteristic curve (AUROC) and the false positive rate at 95% recall (FRP95) are computed between $\mathcal{D}_{\text{out}}^{\text{test}}$ test and $\mathcal{D}_{\text{in}}^{\text{test}}$. Below, we present the used OOD detection scores, given a pretrained backbone model g .

1-NN. For the unsupervised evaluations, we use the maximum of the cosine similarity (Sun et al., 2022) between a test image x' and $x_i \in \mathcal{D}_{\text{in}}^{\text{train}} = \{x_1, x_2, \dots, x_N\}$ as an OOD score:

$$s_{\text{NN}}(x') = \max_i \text{sim}(g(x'), g(x_i)), \quad (1)$$

where $\text{sim}(\cdot)$ is the cosine similarity and N the number of $\mathcal{D}_{\text{in}}^{\text{train}}$ samples.

Mahalanobis distance (MD). The MD can be either applied directly on the feature space of the pretrained model, $z_i = g(x_i)$, or on the trained linear head, $z_i = h(g(x_i))$. However, MD assumes that the in-distribution labels $y_i \in \{y_1, \dots, y_N\}$ are available. We denote the class index $c \in \{1, \dots, C\}$, with C being the number of \mathcal{D}_{in} classes and N_c the number of samples in class c . For each class c , we fit a Gaussian distribution to the representations z (Lee et al., 2018). Specifically, we first compute the per-class mean $\mu_c = \frac{1}{N_c} \sum_{i:y_i=c} z_i$ and a shared covariance matrix

$$\Sigma = \frac{1}{N} \sum_{c=1}^C \sum_{i:y_i=c} (z_i - \mu_c)(z_i - \mu_c)^\top. \quad (2)$$

The Mahalanobis score is then computed for each test sample as

$$\text{MD}_c(z') = (z' - \mu_c)\Sigma^{-1}(z' - \mu_c)^\top, \quad (3)$$

$$s_{\text{MD}}(x') = -\min_c \text{MD}_c(z'). \quad (4)$$

MD can also be applied with cluster-wise means, for instance, using the k -means cluster centers computed on the feature space of g (Sehwag et al., 2021). We denote this score as k -means MD and use the number of ground truth \mathcal{D}_{in} classes to compute the cluster centers.

Relative Mahalanobis distance (RMD). Given the in-distribution mean $\mu_0 = \frac{1}{N} \sum_i z_i$, we additionally compute $\Sigma_0 = \frac{1}{N} \sum_i (z_i - \mu_0)(z_i - \mu_0)^\top$ to compute MD_0 analogously to Eq. (3). Subsequently, the RMD score Ren et al. (2021) can be defined as

$$s_{\text{RMD}}(x') = -\min_c (\text{MD}_c(z') - \text{MD}_0(z')). \quad (5)$$

Energy. As in Liu et al. (2020), negative free energy is computed over the logits z of an \mathcal{D}_{in} classifier as

$$s_{\text{energy}}(x') = T \cdot \log \sum_i^C e^{z'_i/T}, \quad (6)$$

where $T = 1$ is a temperature hyperparameter.

3.3 Pseudo-Label Probing (PLP) using CLIP’s textual encoder

The pseudo-MSP baseline. Ming et al. (2022) proposed a simple visual OOD detection method to leverage CLIP by feeding the \mathcal{D}_{in} class names to CLIP’s text encoder. The resulting text representations are utilized to compute the cosine similarities for each test image, and then the maximum softmax probability (MSP) is computed as an OOD score. We use pseudo-MSP as a baseline.

PLP. We propose a simple method called *pseudo-label probing* (PLP) that extends Ming et al. (2022) by first computing the indices corresponding to the maximum image-text similarity to derive a pseudo-label for each $\mathcal{D}_{\text{in}}^{\text{train}}$ image. A linear layer is then trained with the derived pseudo-labels on the features of g and evaluated using the RMD or energy score, namely $PLP + RMD$ and $PLP + Energy$. PLP remains OOD data-agnostic and assumes no prior information on \mathcal{D}_{out} while training a linear layer adds minimal overhead compared to pseudo-MSP. PLP is conceptually similar to self-training Xie et al. (2020). Differently from standard self-training, we only train a linear layer using the text-based prototype that is closest to each \mathcal{D}_{in} image in feature space derived from the textual encoder of CLIP. The obtained text-based prototypes are treated as pseudo-labels, and a linear mapping is learned from the features of g to the \mathcal{D}_{in} classes.

Similarly, we consider supervised linear probing as an alternative to the existing paradigm of fine-tuning visual feature extractors. Probing refers to training a linear head on the features of the backbone g , using the $\mathcal{D}_{\text{in}}^{\text{train}}$ labels and acts as an upper bound for PLP. Subsequently, RMD or Energy is computed. This is in contrast to existing approaches (Fort et al., 2021; Huang & Li, 2021) that typically fine-tune the visual backbone, which is significantly slower, computationally more expensive, and may lead to catastrophic forgetting (Kemker et al., 2018).

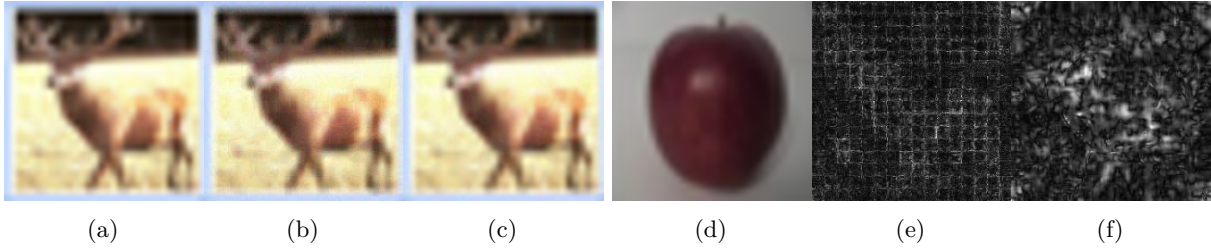


Figure 2: **Generating an adversarial OOD example of a deer that is close enough in the feature space to an in-distribution image of an apple.** From left to right: a) the original OOD image from the CIFAR10 test set, b) the adversarial example without smoothing, c) the adversarial example with smoothing, d) the randomly sampled in-distribution target image from CIFAR100, e) the per-pixel Euclidean distance between the original image and perturbed image, and f) the distance between the original and the smoothly perturbed image.

Method	iNaturalist Plants		OOD Dataset				Texture		NINCO	
	FPR95↓	AUROC↑	SUN	SUN	IN-O	IN-O	FPR95↓	AUROC↑	FPR95↓	AUROC↑
CLIP ViT-B										
Ming et al. (2022)	30.91	94.61	37.59	92.57	-	-	57.77	86.11	-	-
Pseudo-MSP [†]	52.15	89.55	40.34	91.93	78.20	79.47	55.36	86.82	83.09	72.44
PLP + Energy	47.70	93.36	58.15	88.69	79.00	80.72	54.63	86.44	81.93	75.65
CLIP ViT-L										
Ming et al. (2022)	28.38	94.95	29.00	94.14	-	-	59.88	84.88	-	-
Pseudo-MSP [†]	48.30	90.99	29.83	93.91	72.15	81.49	57.93	85.42	74.72	78.47
PLP + Energy	27.24	95.40	44.99	91.05	64.70	85.81	46.75	88.22	71.95	83.83
CLIP ViT-H (LAION-2B)										
Pseudo-MSP [†]	60.35	90.45	42.92	91.50	59.65	87.00	46.95	89.67	74.24	82.99
PLP + Energy	48.61	93.02	40.90	91.78	52.50	89.24	35.00	91.96	71.9	84.88
CLIP ViT-G (LAION-2B)										
Pseudo-MSP [†]	56.49	90.55	38.69	92.75	55.50	88.11	46.95	89.70	71.30	83.38
PLP + Energy	23.51	96.01	34.41	92.90	42.80	91.39	30.38	92.74	59.32	88.65

Table 3: **OOD detection performance metrics using CLIP models and label names for ImageNet-1K as in-distribution.** We report the best metric in bold across different ViTs. The symbol [†] indicates our reproduction of Ming et al. (2022). Crucially, we used the official weights from Radford et al. (2021) while Ming et al. used the weights provided by Hugging Face trained on different web-crawled data, which justifies the discrepancy between the reported results.

3.4 Feature-based adversarial OOD data manipulation

The unsupervised OOD detection performance of CLIP ViT-G, combined with its known classification robustness against natural distribution shifts, raises the question of whether these models are also adversarially robust OOD detectors. To answer this question, we develop an adversarial OOD data manipulation method that matches image features. In particular, for a test image $x' \in \mathcal{D}_{\text{out}}^{\text{test}}$, we randomly choose an in-distribution image $x \in \mathcal{D}_{\text{in}}^{\text{train}}$ as the target. In contrast to existing adversarial attacks (Azizmalayeri et al., 2022; Chen et al., 2020a) that maximize the OOD scores directly, we create an adversarial perturbation ρ with the same dimensions as x' that maximizes the cosine similarity between the in-distribution feature $g(x)$ and $g(x' + \rho)$. Our method targets feature similarities, and it is thus more general as it affects all OOD detection scores. We use the Adam optimizer to compute ρ by minimizing $-\text{sim}(g(x), g(x' + \rho))$, starting with Gaussian noise $\rho \sim \mathcal{N}(0, 10^{-3})$ and clipping $x' + \rho$ to the pixel range $[0, 1]$ after every update step, similar to Yin et al. (2021). We emphasize that we do not directly restrict the perturbation size and only limit the number of steps, as opposed to Yin et al. (2021).

We experimentally observe that in the case of ViTs, the perturbations are quite visible along the edges of the transformer patches (Fig. 2). To create more natural appearing adversarial examples, we enforce the

smoothness of the perturbation by regularizing the allowed perturbation difference between neighboring pixels. We compute the image gradient $\partial\rho/\partial h$ and $\partial\rho/\partial w$ in the horizontal and vertical direction, respectively. The image gradients have the same shape as the image, $3 \times H \times W$, and we define the regularization term as

$$\ell_{\text{smooth}}(\rho) = \frac{1}{3HW} \sum_{ijk} \left(\frac{\partial\rho}{\partial h} \right)_{ijk}^2 + \left(\frac{\partial\rho}{\partial w} \right)_{ijk}^2, \quad (7)$$

where i, j, k run over image dimensions. We then minimize the loss

$$\ell_{\text{adv}} = -\text{sim}(g(x), g(x' + \rho)) + \lambda \ell_{\text{smooth}}(\rho), \quad (8)$$

with respect to the perturbation ρ , where λ is a hyperparameter. During the evaluation, we remove the chosen target image, x , from $\mathcal{D}_{\text{in}}^{\text{train}}$ to show that the adversarial example, $x' + \rho$, cannot be detected as OOD from the remaining in-distribution examples. As a proof of concept, we create two adversarial OOD datasets¹ for the CIFAR100 \rightarrow CIFAR10 benchmark, namely CIFAR10-A ($\lambda = 0$) and its smoothed version CIFAR10-AS ($\lambda > 0$). The generation of an adversarial example is shown in Fig. 2. More adversarial examples can be found in the supplementary material.

3.5 Experimental evaluations

First, we benchmark 25 publicly available pretrained models on common ImageNet and CIFAR OOD detection benchmarks, as illustrated in Fig. 1. Second, we compare PLP against the aforementioned baselines on ImageNet benchmarks in Tab. 3. For a fair comparison with Ming et al. (2022), we use the CLIP ViT-B and ViT-L trained on OpenAI-400M Radford et al. (2021), but also report results with the recently released CLIP ViT-G trained on LAION-2B (Cherti et al., 2022). In contrast to Huang & Li (2021), we remove the Places OOD subset due to its high class overlap of 59.5% with ImageNet (Bitterwolf et al., 2023); instead, we add IN-O and NINCO. Third, in Tab. 4, we compare linear probing on CLIP’s visual representations to standard supervised fine-tuning for OOD detection. Fourth, in Tab. 5, we conduct further OOD detection evaluations with CLIP ViT-G, based on the availability of \mathcal{D}_{in} class names or (few-shot) labeled images and different detection scores. In Tab. 6, we compare linear probing to fine-tuning for ImageNet-21K pretrained models. Finally, we study the robustness against the adversarially created OOD samples (CIFAR10-A, CIFAR10-AS) using CIFAR100 as \mathcal{D}_{in} .

3.6 Implementation details

Since probing and PLP only train a linear layer on precomputed representations, it is more scalable and significantly faster than fine-tuning while having minimal overhead compared to pseudo-MSP. We used the Adam optimizer (Kingma & Ba, 2014) with a mini-batch size of 256 for CIFAR10 and CIFAR100 and 8192 for ImageNet and trained for 100 epochs with a weight decay of 10^{-3} . The learning rate is set to $10^{-3} \cdot (\text{mini-batch size})/256$ with a linear warm-up over the first ten epochs and cosine decay after that. All the experiments were carried out in a single NVIDIA A100 with 40GB VRAM. Moreover, we emphasize that the standard deviation of probing and PLP is less than 0.01%, measured over 10 independent runs. To create the adversarial datasets CIFAR10-A and CIFAR10-AS, we perform 250 steps with the Adam optimizer with a learning rate of 10^{-3} on 1K OOD images. We set λ to $5 \cdot 10^3$ when applying smoothing (Eq. 8).

4 Experimental results

Unsupervised OOD detection. In Fig. 1, we initially investigate whether there is a connection between the $\mathcal{D}_{\text{in}}^{\text{test}}$ classification accuracy and unsupervised OOD detection AUROC by benchmarking 25 feature extractors. Out of them, CLIP models exhibit the strongest correlation (R^2 coefficient ≥ 0.92) independent of their network architecture (i.e. ConvNext, ViTs, etc). CLIP’s best instances (ViT-G, ConvNext-XXL) are currently the best-performing unsupervised OOD detectors, aligning with recent results from Galil et al. (2023). The features of CLIP ViT-G even outperform the ones from supervised training on ImageNet as \mathcal{D}_{in} .

¹<https://drive.google.com/drive/folders/1pYGEPQwagRzdKIPqMQv7sRH6C9MV5vNF>

Method	iNaturalist Plants		OOD Dataset				Texture		NINCO	
	FPR95↓	AUROC↑	SUN		Places		FPR95↓	AUROC↑	FPR95↓	AUROC↑
CLIP ViT-B										
Finetune + MSP	36.80	90.49	60.53	81.72	63.29	80.54	54.42	82.60	63.70	80.94
Probing + Energy	24.36	95.72	50.30	90.03	50.26	88.60	50.97	88.10	78.31	79.23
CLIP ViT-L										
Finetune + MSP	31.33	91.90	51.33	84.97	55.68	82.90	48.68	84.52	56.79	84.27
Probing + Energy	8.65	97.89	41.42	91.91	43.05	90.81	44.14	90.27	67.05	86.32
CLIP ViT-H (LAION-2B)										
Finetune + MSP	26.70	92.90	49.19	85.69	54.51	83.28	46.66	84.70	55.48	83.90
Probing + Energy	6.46	98.28	32.42	93.47	38.89	91.68	26.45	93.93	55.39	89.79
CLIP ViT-G (LAION-2B)										
Probing + Energy	6.29	98.27	32.21	93.27	37.16	92.02	24.63	94.31	49.35	90.4

Table 4: **Supervised OOD detection performance on ImageNet-1K using CLIP: linear probing outperforms fine-tuning on average, especially for larger-scale models, while being computationally cheaper and significantly faster to train.** The best method for each model architecture is bolded, excluding CLIP ViT-G. The reported results from fine-tuning are based on our evaluations using publicly available CLIP weights fine-tuned on ImageNet-1K from *timm* Wightman (2019).

Moreover, we observe that when the $\mathcal{D}_{\text{pretrain}}$ is different from \mathcal{D}_{in} (CIFAR benchmarks), a positive correlation can still be identified for self-supervised and supervised models pretrained on ImageNet ($R^2 = 0.82$), yet not as strong as CLIP ($R^2 = 0.95$).

Large-scale OOD detection with access to class names. We report absolute gains and AUROC scores. In Tab. 3, we compare pseudo-MSP, based on our reproduction of Ming et al. (2022), to PLP on all five large-scale benchmarks and find an average improvement of 2.81%, 1.85%, 3.44% AUROC for CLIP ViT-L, ViT-H, and ViT-G, respectively. The reported gains are computed using the energy score as it was slightly superior to RMD on average and significantly faster to compute. Interestingly, PLP has consistent improvements on the newly proposed NINCO dataset, wherein all samples have been visually verified to be semantically different from \mathcal{D}_{in} , with an average AUROC gain of 3.93% across CLIP models. We highlight that the discrepancy between our reproduction and the reported results of Ming et al. (2022) using ViT-B and ViT-L is due to different CLIP weights: the authors used weights provided by Hugging Face trained on different web-crawled data. In contrast, we used the official weights from Radford et al. (2021).

Large-scale supervised OOD detection. As shown in Tab. 4, fine-tuning CLIP models is often unnecessary for supervised OOD detection. More precisely, probing on larger models such as CLIP ViT-H consistently outperforms fine-tuning by a large margin of 7.34% on average. The performance discrepancy of CLIP ViT-L on Places and SUN compared to the other benchmarks is partially attributed to the class overlap. By contrast, iNaturalist, Texture, and NINCO are sufficiently disjoint from ImageNet in terms of \mathcal{D}_{in} class overlap.

Adversarial OOD detection robustness. By evaluating CLIP ViT-G on the introduced CIFAR100→CIFAR10-A benchmark, we found that it is possible to drop the AUROC score from 87.6% →50.3% using 1-NN and 94.2%→49.5% using pseudo-MSP. Introducing the smoothness restriction (Eq. (8)) degrades performance to 55.8% and 51.9% AUROC on CIFAR100→CIFAR10-AS using 1-NN and pseudo-MSP, respectively. Note that an AUROC score of 50% is a random guess’s score, meaning that CLIP ViT-G performs slightly better than a random guess.

Ablation study for CLIP ViT-G for all OOD detection setups. In Tab. 5, we conduct additional experimental evaluations using CLIP ViT-G for all three OOD detection scenarios (unsupervised, class names are available, supervised). In the unsupervised case, k -means + MD yields an inferior AUROC compared to 1-NN, precisely lower by 6.8% on average. By incorporating the \mathcal{D}_{in} class names using CLIP’s text encoder, we find that the PLP consistently outperforms pseudo-MSP with a mean improvement of 3.16% and 2.63% over PLP+RMD and PLP+Energy respectively. In the supervised scenario, we highlight that RMD is a strong baseline, surpassing MD by 10.75% AUROC on average, while our PLP+Energy marginally improves RMD by 0.47%. MSP is constantly the worst choice as an OOD detection score after linear probing.

CLIP ViT-G/14	\mathcal{D}_{in} labels/names	$\mathcal{D}_{\text{in}}:\text{CIFAR100}$ $\mathcal{D}_{\text{out}}:\text{CIFAR10}$	CIFAR10 CIFAR100	ImageNet IN-O	ImageNet NINCO
k -means MD	\times/\times	72.8	89.5	87.6	80.7
1-NN	\times/\times	87.6	98.2	88.0	84.0
Pseudo-MSP	\times/\checkmark	94.2	97.3	88.1	83.4
PLP + MSP	\times/\checkmark	92.7	97.9	86.6	86.7
PLP + RMD	\times/\checkmark	97.1	98.3	91.9	88.4
PLP + Energy	\times/\checkmark	95.0	98.5	91.4	88.7
MD	\checkmark/\checkmark	73.1	91.1	88.1	81.5
RMD	\checkmark/\checkmark	96.3	98.8	92.4	89.3
Few-shot $p = 10$ + MSP	\checkmark/\checkmark	89.4	96.5	88.1	84.8
Few-shot $p = 10$ + Energy	\checkmark/\checkmark	90.9	96.6	90.8	83.0
Probing + MSP	\checkmark/\checkmark	94.1	98.7	88.1	89.1
Probing + RMD	\checkmark/\checkmark	97.3	98.8	92.5	89.5
Probing + Energy	\checkmark/\checkmark	96.3	99.1	92.9	90.4

Table 5: OOD detection AUROCs (%) for multiple evaluations and scores using CLIP ViT-G/14 trained on LAION-2B.

	Finetuned on \mathcal{D}_{in}	$\mathcal{D}_{\text{in}}:\text{IN1K}$ $\mathcal{D}_{\text{out}}:\text{NINCO}$	IN1K IN-O	CIFAR100 CIFAR10	CIFAR10 CIFAR100
ConvNext-B	\times	95.4	94.9	93.0	98.0
ConvNext-B	\checkmark	88.8	85.8	91.3*	96.3*
ViT-L	\times	95.2	95.3	89.8	94.3
ViT-L	\checkmark	91.3	92.1	97.9*	98.5*
ResNet50+ViT-B	\times	95.9	95.8	89.2	96.6
ResNet50+ViT-B	\checkmark	92.9	92.1	96.2*	98.5*

Table 6: Comparing the OOD detection AUROC (%) of ImageNet-21K pretrained models: linear probing versus fine-tuning. We use publicly available models with and without fine-tuning on ImageNet from *timm* and evaluate them using the energy score. Following Fort et al. (2021), we use the MD on CIFAR fine-tuned models (indicated with an asterisk), which is inefficient at the scale of ImageNet.

5 Discussion

Pixel-related features in CLIP’s learned representations. Similar to Mao et al. (2023) for image classification, the OOD detection performance close to a random guess demonstrates that even the top-performing CLIP models trained on billion-scale image-text pairs can be fooled by a visual signal manipulation that is invisible to humans. This finding gives further evidence that besides label-related features, (local) pixel information affects the learned representations and needs to be explored in greater depth (Park et al., 2023; Dravid et al., 2023). Another possible research avenue is how adversarial OOD samples transfer between different feature extractors, which is left for future work.

Does PLP improve $\mathcal{D}_{\text{in}}^{\text{test}}$ accuracy? By comparing the $\mathcal{D}_{\text{in}}^{\text{test}}$ accuracy on ImageNet of the trained head with the pseudo-labels versus the zero-shot classification of CLIP ViT-G, we found a minor accuracy improvement of 0.5% on ImageNet. However, accuracies deteriorate for CLIP ViT-B and CLIP ViT-L on average, which suggests that their \mathcal{D}_{in} text-based pseudo-labels have less true positives. The fact that PLP improves the OOD detection performance (compared to pseudo-MSP) without significantly increasing $\mathcal{D}_{\text{in}}^{\text{test}}$ accuracy is a new direction left for future work. Another interesting avenue is whether the text-based pseudo-labels from CLIP can be used with other, possibly smaller-scale, visual feature extractors.

Does linear probing lead to similar OOD detection performance compared to fine-tuning for ImageNet-21K pretrained models? In Tab. 6, we compare linear probing versus fine-tuning for 3 publicly

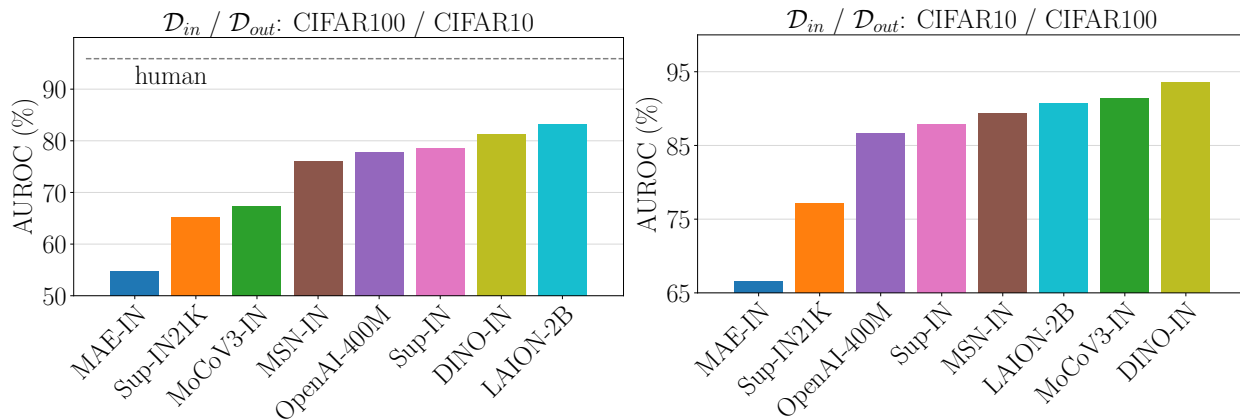


Figure 3: AUROC values for unsupervised OOD detection using ViT-B/16 pretrained on different datasets (IN, IN-21K, OpenAI-400M, LAION-2B) and pretext tasks. IN indicates ImageNet. The performance of CLIP on LAION-2B is bottlenecked by the model size as reported in Cherti et al. (2022) and larger networks are needed when scaling up to billion-scale datasets. The horizontal line indicates human-level performance, as reported in Fort et al. (2021).

available models, where there is a corresponding fine-tuned model on ImageNet. Even though fine-tuning is the standard practice in supervised OOD detection Fort et al. (2021), the obtained results indicate that it performs inferior to linear probing on the ImageNet OOD-related benchmarks even for ImageNet-21K pretrained models. Fine-tuning is, however, still the best approach on the small-scale OOD benchmarks (e.g. CIFAR10 \rightarrow CIFAR100), given ImageNet21K pretraining. This explains why a simple and scalable approach such as probing may have been overlooked. As suggested by Huang & Li (2021), we confirm that OOD detection approaches tested on small-scale benchmarks do not always translate effectively into larger-scale setups, where simpler methods need to be revisited. Combined with the results from Tab. 4, we validate that the OOD-related information is readily available on large-scale foundational models, as recently stated in Inkawhich et al. (2023); Oquab et al. (2023).

Is the choice of the best feature extractor consistent for smaller-sized models? Not in the scale of ViT-B and CIFAR benchmarks. In Fig. 3, we keep the model architecture fixed (ViT-B) and visualize the unsupervised OOD detection performance (1-NN) for different datasets (ImageNet, ImageNet21K, OpenAI-400M, LAION-2B) and pretraining types (CLIP, supervised, self-supervised). The rationale behind evaluating on the CIFAR-based benchmarks is to focus on feature transferability. We highlight that large pretraining datasets such as LAION-2B are bottlenecked by the model size of ViT-B as explained in Cherti et al. (2022). Unlike Fig. 1, we show that the ranking of backbones is not always consistent between different \mathcal{D}_{in} and \mathcal{D}_{out} at this scale. Finally, DINO ViT-B surpasses supervised ImageNet pretraining on both benchmarks, outlining the transferability of features of self-supervised methods, which is consistent with the results of Ericsson et al. (2021); Naseer et al. (2021); Adaloglou et al. (2023).

6 Conclusion

This work presented a thorough experimental study by leveraging pretrained models for visual OOD detection, focusing on CLIP. It was demonstrated that CLIP models are powerful unsupervised OOD detectors, outperforming even \mathcal{D}_{in} supervised models on large-scale OOD detection benchmarks. A fast, simple, OOD data-agnostic, and scalable method called PLP that trains a linear layer based on \mathcal{D}_{in} text-based pseudo-labels was introduced. PLP outperformed the previous state-of-the-art (pseudo-MSP) for most CLIP models and ImageNet-based benchmarks while substantially improving the larger architectures (i.e. ViT-G achieves a mean AUROC gain of 3.4%). Furthermore, it was demonstrated that probing can replace the costly fine-tuning on CLIP and even ImageNet-21K models on large-scale benchmarks, where CLIP ViT-H exhibited an average AUROC improvement of 7.3%. Finally, a novel feature-based adversarial OOD data manipulation

method was introduced, which pointed to the fact that billion-scale feature extractors (CLIP ViT-G) are vulnerable to adversarial OOD attacks.

References

- Nikolas Adaloglou, Felix Michels, Hamza Kalisch, and Markus Kollmann. Exploring the limits of deep image clustering using pretrained models. *arXiv preprint arXiv:2303.17896*, 2023.
- Dario Amodei, Chris Olah, Jacob Steinhardt, Paul Christiano, John Schulman, and Dan Mané. Concrete problems in ai safety. *arXiv preprint arXiv:1606.06565*, 2016.
- Mahmoud Assran, Mathilde Caron, Ishan Misra, Piotr Bojanowski, Florian Bordes, Pascal Vincent, Armand Joulin, Mike Rabbat, and Nicolas Ballas. Masked siamese networks for label-efficient learning. In Shai Avidan, Gabriel J. Brostow, Moustapha Cissé, Giovanni Maria Farinella, and Tal Hassner (eds.), *Computer Vision - ECCV 2022 - 17th European Conference, Tel Aviv, Israel, October 23-27, 2022, Proceedings, Part XXXI*, volume 13691 of *Lecture Notes in Computer Science*, pp. 456–473. Springer, 2022. doi: 10.1007/978-3-031-19821-2_26. URL https://doi.org/10.1007/978-3-031-19821-2_26.
- Mohammad Azizmalayeri, Arshia Soltani Moakar, Arman Zarei, Reihaneh Zohrabi, Mohammad Taghi Manzuri, and Mohammad Hossein Rohban. Your out-of-distribution detection method is not robust! In Alice H. Oh, Alekh Agarwal, Danielle Belgrave, and Kyunghyun Cho (eds.), *Advances in Neural Information Processing Systems*, 2022. URL <https://openreview.net/forum?id=YUEP3ZmkL1>.
- Lucas Beyer, Pavel Izmailov, Alexander Kolesnikov, Mathilde Caron, Simon Kornblith, Xiaohua Zhai, Matthias Minderer, Michael Tschannen, Ibrahim Alabdulmohsin, and Filip Pavetic. Flexivit: One model for all patch sizes. In *Proceedings of the IEEE/CVF Conference on Computer Vision and Pattern Recognition*, pp. 14496–14506, 2023.
- Julian Bitterwolf, Maximilian Mueller, and Matthias Hein. In or out? fixing imagenet out-of-distribution detection evaluation. In *ICML, 2023*. URL <https://proceedings.mlr.press/v202/bitterwolf23a.html>.
- Rishi Bommasani, Drew A Hudson, Ehsan Adeli, Russ Altman, Simran Arora, Sydney von Arx, Michael S Bernstein, Jeannette Bohg, Antoine Bosselut, Emma Brunskill, et al. On the opportunities and risks of foundation models. *arXiv preprint arXiv:2108.07258*, 2021.
- Mathilde Caron, Hugo Touvron, Ishan Misra, Hervé Jégou, Julien Mairal, Piotr Bojanowski, and Armand Joulin. Emerging properties in self-supervised vision transformers. In *Proceedings of the IEEE/CVF International Conference on Computer Vision*, pp. 9650–9660, 2021.
- Jiefeng Chen, Yixuan Li, Xi Wu, Yingyu Liang, and Somesh Jha. Robust out-of-distribution detection for neural networks. *arXiv preprint arXiv:2003.09711*, 2020a.
- Ting Chen, Simon Kornblith, Mohammad Norouzi, and Geoffrey Hinton. A simple framework for contrastive learning of visual representations. In *International conference on machine learning*, pp. 1597–1607. PMLR, 2020b.
- Xinlei Chen, Saining Xie, and Kaiming He. An empirical study of training self-supervised vision transformers. In *Proceedings of the IEEE/CVF International Conference on Computer Vision*, pp. 9640–9649, 2021.
- Mehdi Cherti, Romain Beaumont, Ross Wightman, Mitchell Wortsman, Gabriel Ilharco, Cade Gordon, Christoph Schuhmann, Ludwig Schmidt, and Jenia Jitsev. Reproducible scaling laws for contrastive language-image learning. *arXiv preprint arXiv:2212.07143*, 2022.
- Mircea Cimpoi, Subhransu Maji, Iasonas Kokkinos, Sammy Mohamed, and Andrea Vedaldi. Describing textures in the wild. In *Proceedings of the IEEE conference on computer vision and pattern recognition*, pp. 3606–3613, 2014.

-
- Niv Cohen, Ron Abutbul, and Yedid Hoshen. Out-of-distribution detection without class labels. In *Computer Vision–ECCV 2022 Workshops: Tel Aviv, Israel, October 23–27, 2022, Proceedings, Part II*, pp. 101–117. Springer, 2023.
- Mostafa Dehghani, Josip Djolonga, Basil Mustafa, Piotr Padlewski, Jonathan Heek, Justin Gilmer, Andreas Steiner, Mathilde Caron, Robert Geirhos, Ibrahim Alabdulmohsin, et al. Scaling vision transformers to 22 billion parameters. *arXiv preprint arXiv:2302.05442*, 2023.
- Jia Deng, Wei Dong, Richard Socher, Li-Jia Li, Kai Li, and Li Fei-Fei. Imagenet: A large-scale hierarchical image database. In *2009 IEEE conference on computer vision and pattern recognition*, pp. 248–255. Ieee, 2009.
- Alexey Dosovitskiy, Lucas Beyer, Alexander Kolesnikov, Dirk Weissenborn, Xiaohua Zhai, Thomas Unterthiner, Mostafa Dehghani, Matthias Minderer, Georg Heigold, Sylvain Gelly, Jakob Uszkoreit, and Neil Houlsby. An image is worth 16x16 words: Transformers for image recognition at scale. In *International Conference on Learning Representations*, 2021. URL <https://openreview.net/forum?id=YicbFdNTTy>.
- Amil Dravid, Yossi Gandelsman, Alexei A Efros, and Assaf Shocher. Rosetta neurons: Mining the common units in a model zoo. In *Proceedings of the IEEE/CVF International Conference on Computer Vision*, pp. 1934–1943, 2023.
- Linus Ericsson, Henry Gouk, and Timothy M Hospedales. How well do self-supervised models transfer? In *Proceedings of the IEEE/CVF Conference on Computer Vision and Pattern Recognition*, pp. 5414–5423, 2021.
- Sepideh Esmailpour, Bing Liu, Eric Robertson, and Lei Shu. Zero-shot out-of-distribution detection based on the pre-trained model clip. In *Proceedings of the AAAI conference on artificial intelligence*, volume 36, pp. 6568–6576, 2022.
- Stanislav Fort, Jie Ren, and Balaji Lakshminarayanan. Exploring the limits of out-of-distribution detection. *Advances in Neural Information Processing Systems*, 34:7068–7081, 2021.
- Ido Galil, Mohammed Dabbah, and Ran El-Yaniv. A framework for benchmarking class-out-of-distribution detection and its application to imagenet. In *The Eleventh International Conference on Learning Representations*, 2023. URL <https://openreview.net/forum?id=Iuubb9W6Jtk>.
- Robert Geirhos, Jörn-Henrik Jacobsen, Claudio Michaelis, Richard Zemel, Wieland Brendel, Matthias Bethge, and Felix A Wichmann. Shortcut learning in deep neural networks. *Nature Machine Intelligence*, 2(11): 665–673, 2020.
- Spyros Gidaris, Praveer Singh, and Nikos Komodakis. Unsupervised representation learning by predicting image rotations. In *International Conference on Learning Representations*, 2018. URL <https://openreview.net/forum?id=S1v4N210->.
- Ian J. Goodfellow, Jonathon Shlens, and Christian Szegedy. Explaining and harnessing adversarial examples. In Yoshua Bengio and Yann LeCun (eds.), *3rd International Conference on Learning Representations, ICLR 2015, San Diego, CA, USA, May 7-9, 2015, Conference Track Proceedings*, 2015. URL <http://arxiv.org/abs/1412.6572>.
- Chuan Guo, Geoff Pleiss, Yu Sun, and Kilian Q Weinberger. On calibration of modern neural networks. In *International conference on machine learning*, pp. 1321–1330. PMLR, 2017.
- Kaiming He, Xiangyu Zhang, Shaoqing Ren, and Jian Sun. Deep residual learning for image recognition. In *Proceedings of the IEEE conference on computer vision and pattern recognition*, pp. 770–778, 2016.
- Kaiming He, Ross Girshick, and Piotr Dollár. Rethinking imagenet pre-training, 2019.
- Dan Hendrycks and Thomas Dietterich. Benchmarking neural network robustness to common corruptions and perturbations. In *International Conference on Learning Representations*, 2019. URL <https://openreview.net/forum?id=HJz6tiCqYm>.

-
- Dan Hendrycks and Kevin Gimpel. A baseline for detecting misclassified and out-of-distribution examples in neural networks. In *International Conference on Learning Representations*, 2017. URL <https://openreview.net/forum?id=Hkg4TI9x1>.
- Dan Hendrycks, Mantas Mazeika, and Thomas Dietterich. Deep anomaly detection with outlier exposure. In *International Conference on Learning Representations*, 2019a.
- Dan Hendrycks, Mantas Mazeika, Saurav Kadavath, and Dawn Song. Using self-supervised learning can improve model robustness and uncertainty. *Advances in neural information processing systems*, 32, 2019b.
- Dan Hendrycks, Xiaoyuan Liu, Eric Wallace, Adam Dziedzic, Rishabh Krishnan, and Dawn Song. Pretrained transformers improve out-of-distribution robustness. In *ACL*, pp. 2744–2751, 2020. URL <https://doi.org/10.18653/v1/2020.acl-main.244>.
- Dan Hendrycks, Steven Basart, Norman Mu, Saurav Kadavath, Frank Wang, Evan Dorundo, Rahul Desai, Tyler Zhu, Samyak Parajuli, Mike Guo, et al. The many faces of robustness: A critical analysis of out-of-distribution generalization. In *Proceedings of the IEEE/CVF International Conference on Computer Vision*, pp. 8340–8349, 2021a.
- Dan Hendrycks, Kevin Zhao, Steven Basart, Jacob Steinhardt, and Dawn Song. Natural adversarial examples. In *Proceedings of the IEEE/CVF Conference on Computer Vision and Pattern Recognition*, pp. 15262–15271, 2021b.
- Dan Hendrycks, Steven Basart, Mantas Mazeika, Andy Zou, Joseph Kwon, Mohammadreza Mostajabi, Jacob Steinhardt, and Dawn Song. Scaling out-of-distribution detection for real-world settings. In *Proceedings of the 39th International Conference on Machine Learning*, volume 162 of *Proceedings of Machine Learning Research*, pp. 8759–8773. PMLR, 2022. URL <https://proceedings.mlr.press/v162/hendrycks22a.html>.
- Rui Huang and Yixuan Li. Mos: Towards scaling out-of-distribution detection for large semantic space. In *Proceedings of the IEEE/CVF Conference on Computer Vision and Pattern Recognition*, pp. 8710–8719, 2021.
- Nathan Inkawhich, Gwendolyn McDonald, and Ryan Luley. Adversarial attacks on foundational vision models. *arXiv preprint arXiv:2308.14597*, 2023.
- Ronald Kemker, Marc McClure, Angelina Abitino, Tyler Hayes, and Christopher Kanan. Measuring catastrophic forgetting in neural networks. In *Proceedings of the AAAI conference on artificial intelligence*, volume 32, 2018.
- Prannay Khosla, Piotr Teterwak, Chen Wang, Aaron Sarna, Yonglong Tian, Phillip Isola, Aaron Maschinot, Ce Liu, and Dilip Krishnan. Supervised contrastive learning. *Advances in neural information processing systems*, 33:18661–18673, 2020.
- Diederik Kingma and Jimmy Ba. Adam: A method for stochastic optimization. *International Conference on Learning Representations*, 12 2014.
- Alex Krizhevsky, Geoffrey Hinton, et al. Learning multiple layers of features from tiny images. 2009.
- Kimin Lee, Kibok Lee, Honglak Lee, and Jinwoo Shin. A simple unified framework for detecting out-of-distribution samples and adversarial attacks. *Advances in neural information processing systems*, 31, 2018.
- Shiyu Liang, Yixuan Li, and R. Srikant. Enhancing the reliability of out-of-distribution image detection in neural networks. In *International Conference on Learning Representations*, 2018. URL <https://openreview.net/forum?id=H1VGkIxRZ>.
- Weitang Liu, Xiaoyun Wang, John Owens, and Yixuan Li. Energy-based out-of-distribution detection. *Advances in neural information processing systems*, 33:21464–21475, 2020.

-
- Ze Liu, Yutong Lin, Yue Cao, Han Hu, Yixuan Wei, Zheng Zhang, Stephen Lin, and Baining Guo. Swin transformer: Hierarchical vision transformer using shifted windows. In *Proceedings of the IEEE/CVF international conference on computer vision*, pp. 10012–10022, 2021.
- Zhuang Liu, Hanzi Mao, Chao-Yuan Wu, Christoph Feichtenhofer, Trevor Darrell, and Saining Xie. A convnet for the 2020s. In *Proceedings of the IEEE/CVF Conference on Computer Vision and Pattern Recognition*, pp. 11976–11986, 2022.
- Philipp Liznerski, Lukas Ruff, Robert A. Vandermeulen, Billy Joe Franks, Klaus Robert Muller, and Marius Kloft. Exposing outlier exposure: What can be learned from few, one, and zero outlier images. *Transactions on Machine Learning Research*, 2022. ISSN 2835-8856.
- Stuart Lloyd. Least squares quantization in pcm. *IEEE transactions on information theory*, 28(2):129–137, 1982.
- Dhruv Mahajan, Ross Girshick, Vignesh Ramanathan, Kaiming He, Manohar Paluri, Yixuan Li, Ashwin Bharambe, and Laurens Van Der Maaten. Exploring the limits of weakly supervised pretraining. In *Proceedings of the European conference on computer vision (ECCV)*, pp. 181–196, 2018.
- Chengzhi Mao, Scott Geng, Junfeng Yang, Xin Wang, and Carl Vondrick. Understanding zero-shot adversarial robustness for large-scale models. In *The Eleventh International Conference on Learning Representations*, 2023. URL <https://openreview.net/forum?id=P4bXCawRi5J>.
- Yifei Ming, Ziyang Cai, Jiuxiang Gu, Yiyong Sun, Wei Li, and Yixuan Li. Delving into out-of-distribution detection with vision-language representations. *Advances in Neural Information Processing Systems*, 35: 35087–35102, 2022.
- Sina Mohseni, Arash Vahdat, and Jay Yadawa. Shifting transformation learning for out-of-distribution detection. *arXiv preprint arXiv:2106.03899*, 2021.
- Eric Nalisnick, Akihiro Matsukawa, Yee Whye Teh, Dilan Gorur, and Balaji Lakshminarayanan. Do deep generative models know what they don’t know? In *International Conference on Learning Representations*, 2019. URL <https://openreview.net/forum?id=H1xwNhCcYm>.
- Muhammad Muzammal Naseer, Kanchana Ranasinghe, Salman H Khan, Munawar Hayat, Fahad Shah-baz Khan, and Ming-Hsuan Yang. Intriguing properties of vision transformers. *Advances in Neural Information Processing Systems*, 34:23296–23308, 2021.
- Anh Nguyen, Jason Yosinski, and Jeff Clune. Deep neural networks are easily fooled: High confidence predictions for unrecognizable images. In *2015 IEEE Conference on Computer Vision and Pattern Recognition (CVPR)*, pp. 427–436, 2015. doi: 10.1109/CVPR.2015.7298640.
- Maxime Oquab, Timothée Darcet, Théo Moutakanni, Huy Vo, Marc Szafraniec, Vasil Khalidov, Pierre Fernandez, Daniel Haziza, Francisco Massa, Alaaeldin El-Nouby, et al. Dinov2: Learning robust visual features without supervision. *arXiv preprint arXiv:2304.07193*, 2023.
- Namuk Park, Wonjae Kim, Byeongho Heo, Taekyung Kim, and Sangdoon Yun. What do self-supervised vision transformers learn? In *The Eleventh International Conference on Learning Representations*, 2023. URL <https://openreview.net/forum?id=azCKuYyS74>.
- Hieu Pham, Zihang Dai, Golnaz Ghiasi, Kenji Kawaguchi, Hanxiao Liu, Adams Wei Yu, Jiahui Yu, Yi-Ting Chen, Minh-Thang Luong, Yonghui Wu, et al. Combined scaling for zero-shot transfer learning. *Neurocomputing*, 555:126658, 2023.
- Alec Radford, Jong Wook Kim, Chris Hallacy, Aditya Ramesh, Gabriel Goh, Sandhini Agarwal, Girish Sastry, Amanda Askell, Pamela Mishkin, Jack Clark, et al. Learning transferable visual models from natural language supervision. In *International Conference on Machine Learning*, pp. 8748–8763. PMLR, 2021.

-
- Nima Rafiee, Rahil Gholamipoor, Nikolas Adaloglou, Simon Jaxy, Julius Ramakers, and Markus Kollmann. Self-supervised anomaly detection by self-distillation and negative sampling. In *Artificial Neural Networks and Machine Learning–ICANN 2022: 31st International Conference on Artificial Neural Networks, Bristol, UK, September 6–9, 2022, Proceedings; Part IV*, pp. 459–470. Springer, 2022.
- Tal Reiss, Niv Cohen, Liron Bergman, and Yedid Hoshen. Panda: Adapting pretrained features for anomaly detection and segmentation. In *Proceedings of the IEEE/CVF Conference on Computer Vision and Pattern Recognition*, pp. 2806–2814, 2021.
- Jie Ren, Peter J Liu, Emily Fertig, Jasper Snoek, Ryan Poplin, Mark Depristo, Joshua Dillon, and Balaji Lakshminarayanan. Likelihood ratios for out-of-distribution detection. *Advances in neural information processing systems*, 32, 2019.
- Jie Ren, Stanislav Fort, Jeremiah Liu, Abhijit Guha Roy, Shreyas Padhy, and Balaji Lakshminarayanan. A simple fix to mahalanobis distance for improving near-ood detection. *arXiv preprint arXiv:2106.09022*, 2021.
- Olga Russakovsky, Jia Deng, Hao Su, Jonathan Krause, Sanjeev Satheesh, Sean Ma, Zhiheng Huang, Andrej Karpathy, Aditya Khosla, Michael Bernstein, et al. Imagenet large scale visual recognition challenge. *International journal of computer vision*, 115:211–252, 2015.
- Christoph Schuhmann, Romain Beaumont, Richard Vencu, Cade Gordon, Ross Wightman, Mehdi Cherti, Theo Coombes, Aarush Katta, Clayton Mullis, Mitchell Wortsman, et al. Laion-5b: An open large-scale dataset for training next generation image-text models. *Advances in Neural Information Processing Systems*, 35:25278–25294, 2022.
- Vikash Sehwal, Mung Chiang, and Prateek Mittal. {SSD}: A unified framework for self-supervised outlier detection. In *International Conference on Learning Representations*, 2021. URL <https://openreview.net/forum?id=v5gjXpmR8J>.
- Yiyu Sun, Yifei Ming, Xiaojin Zhu, and Yixuan Li. Out-of-distribution detection with deep nearest neighbors. In *International Conference on Machine Learning*, pp. 20827–20840. PMLR, 2022.
- Christian Szegedy, Wojciech Zaremba, Ilya Sutskever, Joan Bruna, Dumitru Erhan, Ian J. Goodfellow, and Rob Fergus. Intriguing properties of neural networks. In Yoshua Bengio and Yann LeCun (eds.), *2nd International Conference on Learning Representations, ICLR 2014, Banff, AB, Canada, April 14-16, 2014, Conference Track Proceedings*, 2014. URL <http://arxiv.org/abs/1312.6199>.
- Jihoon Tack, Sangwoo Mo, Jongheon Jeong, and Jinwoo Shin. Csi: Novelty detection via contrastive learning on distributionally shifted instances. *Advances in neural information processing systems*, 33:11839–11852, 2020.
- Chuanqi Tan, Fuchun Sun, Tao Kong, Wenchang Zhang, Chao Yang, and Chunfang Liu. A survey on deep transfer learning. In *Artificial Neural Networks and Machine Learning–ICANN 2018: 27th International Conference on Artificial Neural Networks, Rhodes, Greece, October 4-7, 2018, Proceedings, Part III 27*, pp. 270–279. Springer, 2018.
- Hugo Touvron, Matthieu Cord, Alexandre Sablayrolles, Gabriel Synnaeve, and Hervé Jégou. Going deeper with image transformers. In *Proceedings of the IEEE/CVF International Conference on Computer Vision*, pp. 32–42, 2021.
- Grant Van Horn, Oisín Mac Aodha, Yang Song, Yin Cui, Chen Sun, Alex Shepard, Hartwig Adam, Pietro Perona, and Serge Belongie. The inaturalist species classification and detection dataset. In *Proceedings of the IEEE conference on computer vision and pattern recognition*, pp. 8769–8778, 2018.
- Florian Wenzel, Andrea Dittadi, Peter Vincent Gehler, Carl-Johann Simon-Gabriel, Max Horn, Dominik Zietlow, David Kernert, Chris Russell, Thomas Brox, Bernt Schiele, et al. Assaying out-of-distribution generalization in transfer learning. *arXiv preprint arXiv:2207.09239*, 2022.

-
- Ross Wightman. Pytorch image models. <https://github.com/rwightman/pytorch-image-models>, 2019.
- Jim Winkens, Rudy Bunel, Abhijit Guha Roy, Robert Stanforth, Vivek Natarajan, Joseph R Ledsam, Patricia MacWilliams, Pushmeet Kohli, Alan Karthikesalingam, Simon Kohl, et al. Contrastive training for improved out-of-distribution detection. *arXiv preprint arXiv:2007.05566*, 2020.
- Mitchell Wortsman, Gabriel Ilharco, Jong Wook Kim, Mike Li, Simon Kornblith, Rebecca Roelofs, Raphael Gontijo Lopes, Hannaneh Hajishirzi, Ali Farhadi, Hongseok Namkoong, et al. Robust fine-tuning of zero-shot models. In *Proceedings of the IEEE/CVF Conference on Computer Vision and Pattern Recognition*, pp. 7959–7971, 2022.
- Jianxiong Xiao, James Hays, Krista A Ehinger, Aude Oliva, and Antonio Torralba. Sun database: Large-scale scene recognition from abbey to zoo. In *2010 IEEE computer society conference on computer vision and pattern recognition*, pp. 3485–3492. IEEE, 2010.
- Qizhe Xie, Minh-Thang Luong, Eduard Hovy, and Quoc V Le. Self-training with noisy student improves imagenet classification. In *Proceedings of the IEEE/CVF conference on computer vision and pattern recognition*, pp. 10687–10698, 2020.
- Jingkang Yang, Pengyun Wang, Dejian Zou, Zitang Zhou, Kunyuan Ding, Wenxuan Peng, Haoqi Wang, Guangyao Chen, Bo Li, Yiyu Sun, et al. Openood: Benchmarking generalized out-of-distribution detection. *Advances in Neural Information Processing Systems*, 35:32598–32611, 2022.
- Heng Yin, Hengwei Zhang, Jindong Wang, and Ruiyu Dou. Boosting adversarial attacks on neural networks with better optimizer. *Secur. Commun. Networks*, 2021:9983309:1–9983309:9, 2021. doi: 10.1155/2021/9983309. URL <https://doi.org/10.1155/2021/9983309>.
- Jason Yosinski, Jeff Clune, Yoshua Bengio, and Hod Lipson. How transferable are features in deep neural networks? *Advances in neural information processing systems*, 27, 2014.
- Hongjie Zhang, Ang Li, Jie Guo, and Yanwen Guo. Hybrid models for open set recognition. In *Computer Vision–ECCV 2020: 16th European Conference, Glasgow, UK, August 23–28, 2020, Proceedings, Part III 16*, pp. 102–117. Springer, 2020.
- Bolei Zhou, Agata Lapedriza, Aditya Khosla, Aude Oliva, and Antonio Torralba. Places: A 10 million image database for scene recognition. *IEEE transactions on pattern analysis and machine intelligence*, 40(6): 1452–1464, 2017.

A Supplementary material: Adapting Contrastive Language-Image Pretrained (CLIP) Models for Out-of-Distribution Detection

A.1 Additional implementation details

Following Ming et al. (2022), for the text encoder of CLIP, we take the mean of the L2-normalized text representations of the following prompts: “an image of a {label}”, “a photo of a {label}”, “a blurry photo of a {label}”, “a photo of many {label}”, “a photo of the large {label}”, “a photo of the small {label}”. We randomly select $p = 10$ images per class for few-shot probing and take the average AUROC over 5 runs. We set the mini-batch size to 32 for CIFAR100 and 1024 for ImageNet. To enforce reproducibility for our results on Table 6, the corresponding models can be found using the *timm* (version 0.6.12) names Wightman (2019): *vit_large_patch16_224_in21k*, *convnext_base_in22k*, and *vit_base_r50_s16_224_in21k*. We note that probing takes less than 15 minutes on ImageNet on a single GPU.

A.2 Does PLP using an MLP achieve superior results?

We found negligible differences when substituting the linear layer with an MLP, which suggests that a linear mapping to the space of in-distribution classes is sufficient for OOD detection.

A.3 Computational complexity of OOD detection methods.

As reported in Table 6, Fort et al. (2021) used the MD as an OOD score, which is inefficient at the scale of ImageNet and can become prohibitively slow for even larger datasets. Given a feature dimension d and dataset size N , the total time complexity scales linearly with dataset size (for the computation of the covariance matrix) and in cubic time with d due to the inverse calculation of the covariance matrix, resulting in $O(Nd \min(N, d) + d^3) = O(Nd^2 + d^3)$ since $N > d$. We thus conclude that, in addition to the performance metrics, the computational complexities need to be taken into account in future studies to design scalable and efficient OOD detection systems.

A.4 Additional few-shot evaluations on CIFAR100 → CIFAR10

In Fig. 4, we show that even with 1% of the data, we can surpass the zero-shot 1-NN score. RMD applied on the logits seems to be consistently better than MSP.

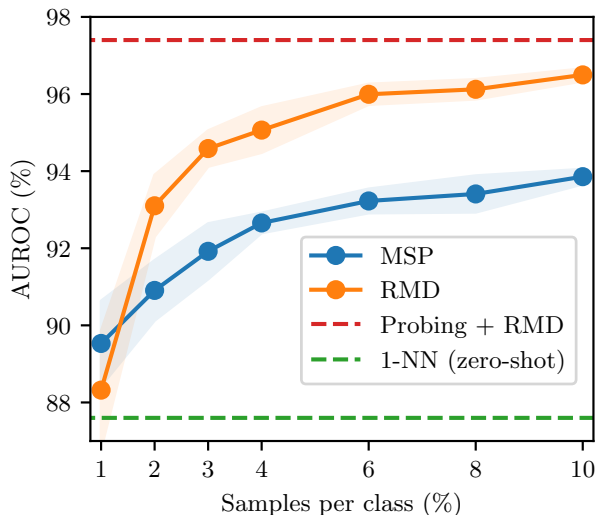


Figure 4: **Few-shot linear probing on CIFAR100 → CIFAR10.** Samples per class (shown as a percentage %) versus OOD detection performance (y -axis).

A.5 Additional adversarial examples

We illustrate more adversarially generated samples using the proposed method in Fig. 5. The created adversarial OOD datasets CIFAR10-A and CIFAR10-AS are publicly available via [this hyperlink](#).

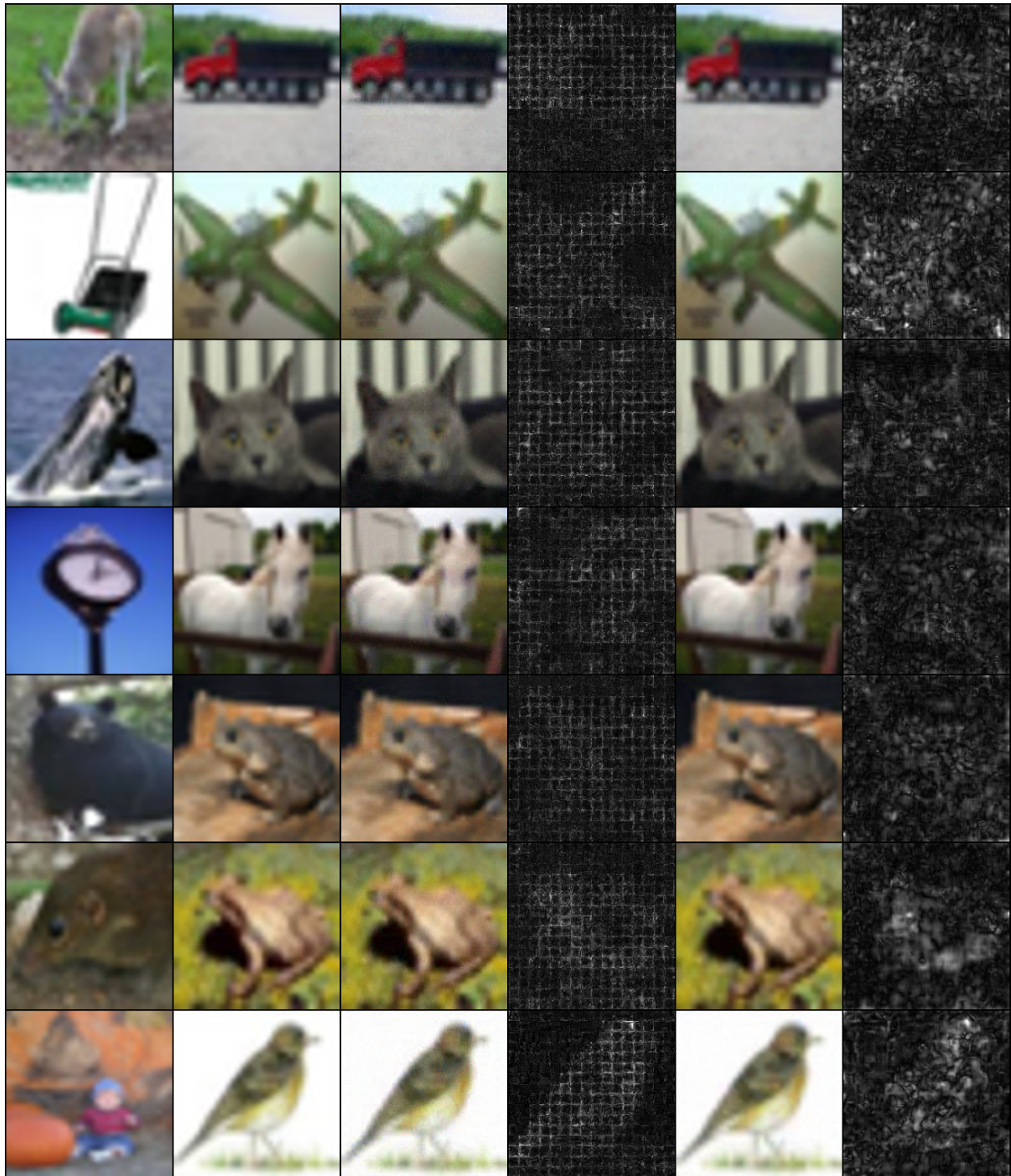


Figure 5: Additional CIFAR10 adversarially manipulated examples for CIFAR100 \rightarrow CIFAR10 OOD detection with (CIFAR10-AS) and without (CIFAR10-A) the smoothing constraint. Columns from *left to right*: target in-distribution image from CIFAR100, original CIFAR10 sample, adversarially manipulated image without smoothing, the Euclidean pixel-wise distance between the original image and perturbed image, adversarial example with smoothing, Euclidean distance.